

DSBP: Data-free and Swift Backdoor Purification for Trustworthy Federated Learning via Multi-teacher Adversarial Distillation

Gaolei Li¹, Jun Wu¹ and Jianhua Li¹ and Yuanyuan Zhao² and Longfei Zheng³

¹ Shanghai Jiao Tong University

² Hangzhou Normal University

³ Ant Group

{gaolei_li, junwuhn, lijh888}@sjtu.edu.cn, yyzhao04@163.com, zlf206411@antgroup.com

Abstract

Federated learning (FL) faces with severe backdoor threats. Due to the inaccessibility of clean samples, the parameter server cannot clean them up in real time even if poisoning features are discovered. Meanwhile, existing backdoor defence methods always require sacrificing model accuracy or increasing communication delay in exchange for better FL trustworthiness, which is unpractical in real scenarios. To address these challenges, we propose a novel data-free and swift backdoor purification (DSBP) scheme based on multi-teacher adversarial distillation, which can effectively erase various backdoor variants in FL. The DSBP treats the purification task as an adversarial game process between knowledge inheritance and backdoor inhibition, with the goal of enforcing the student model to learn the ensemble results of multiple teacher models on reconstructed clean samples, while being insensitive to synthetic poisoned samples. In DSBP, we propose to utilize the self-similarity of poisoned features to optimize the trigger generator, which is essential to accelerate the convergence of DSBP during the adversarial distillation process. We validate that the effectiveness of proposed DSBP by comparing with 4 state-of-the-art defense approaches against 3 backdoor variants on 3 datasets. The average attack success rate can be reduced from 96.6% to 2.3% with only 200 epochs.

1 Introduction

Federated learning (FL) coordinates a large number of distributed clients to complete a global model training task over massive local data samples [Lim *et al.*, 2020]. A typical FL system mainly includes two kinds of entities: 1) clients, which can receive learning tasks and submit model updates; 2) servers, which can aggregate distributed model updates to obtain a global model based on specific rules. Recently, backdoor attacks on FL obtains increasing attention due to the high attack success rate they have achieved [Li *et al.*, 2022]. New backdoor variants in FL render previous backdoor defense methods that aim to do everything possible (i.e., trigger removal, ensemble prediction) at the client side to

disrupt the necessary backdoor implantation conditions uselessly [Hayase *et al.*, 2021]. Firstly, FL infrastructures are often delivered by open-source platforms (such as WeBank FATE, TensorFlow-federated, PaddleFL, etc). Such third-party FL infrastructure offers a venue for new backdoor variants, such as poisoning the pre-trained models [Jia *et al.*, 2022], neuron hijacking [Liu *et al.*, 2018b], and even code poisoning [Bagdasaryan and Shmatikov, 2020]. Secondly, in a real FL scenario, the cost of identifying poisoned samples one by one is very huge. Moreover, since FL does not usually require every node to participate in the training process, it is difficult to determine the deployment location, timing, and scale of existing defense methods [Goldblum *et al.*, 2022]. In terms of backdoor purification methods that target to remove backdoors from the final delivered models [Qiao *et al.*, 2019; Wang *et al.*, 2019; Li *et al.*, 2021; Liu *et al.*, 2021], it’s workflow is often divided into two stages: 1) model diagnosing, 2) model sanitizing. The former stage aims to determine if the suspect model really contains a hidden backdoor [Chen *et al.*, 2019b; Kolouri *et al.*, 2020; Xu *et al.*, 2021]. The model sanitizing stage aims to “forget” hidden backdoors using fine-tuned [Wang *et al.*, 2019], pruned [Liu *et al.*, 2018a], or distilled [Li *et al.*, 2021].

Although many defence methods have been validated to perform reasonably well in experimental settings, three troubles it still should deal with in real-world FL systems: 1) *Lack of adaptability to multiple backdoor variants*. During the whole backdoor purification process, the criteria for model diagnosis is extremely rigid so that it will not work when the adversary changes attack modes [Wang *et al.*, 2019]. In other words, it will suffer from a high misdiagnosis rate. 2) *Hindering the model accuracy*. As the intensity of model purification increases, the backdoor gets weaker. But evaluations in [Yan *et al.*, 2023] show that existing data-driven methods have unacceptable model accuracy degradation (10%) on the CIFAR10 dataset when all employed backdoors are wiped out. In the FL scenario, this degradation will be more sharply.

Our work: We propose a novel data-free swift backdoor purification (DSBP) scheme for trustworthy FL, in which a multi-teacher adversarial distillation (MAD) mechanism is designed to train a clean student model with reconstructed data. In DSBP, two teacher models are used: 1) weak model \mathcal{T}_w at training round r , 2) strong model \mathcal{T}_s at training round $r + k$. The larger r is, the higher the model accuracy is. The

DSBP integrates backdoor detection and sanitation into one adversarial game procedure, where a clean student model \mathcal{S} is obtained by absorbing the knowledge of \mathcal{T}_s and \mathcal{T}_w , while discards hidden backdoors. Given a backdoored model, two mutually-exclusive objectives will be jointly optimizing: 1) *knowledge inheritance*, which maximizes the similarity between the outputs of \mathcal{T}_s and the ensemble results of \mathcal{S} and \mathcal{T}_w over the entire input space, absorbing the knowledge from \mathcal{T}_s and \mathcal{T}_w , and 2) *backdoor inhibition*, which minimizes the expected output change of \mathcal{S} w.r.t. the input change. By jointly optimizing these two objectives based on the MAD mechanism, \mathcal{S}^* finally reaches the desired equilibrium: it inherits the knowledge of \mathcal{T}_s and \mathcal{T}_w (achieving the same accuracy on benign samples), and shows high robustness to malicious samples that can trigger the hidden backdoors in \mathcal{T}_s . Our contributions are summarized as follows:

- We propose a novel wisdom of backdoor purification and create a tool, named as DSBP, which can swiftly cures the backdoored FL model without clean training samples. To the best of our knowledge, DSBP is the fastest and most practical backdoor purification method for real FL systems.
- A multi-teacher adversarial distillation (MAD) mechanism is proposed to optimize an adversarial game procedure, which requires to achieve an equilibrium state between knowledge inheritance and backdoor inhibition. Therein, trigger generator is optimized based on the self-similarity of poisoned features.
- We conduct comprehensive evaluations involving 3 standard image datasets, several different sizes of patched triggers, 4 state of the art backdoor defences, and 3 kinds of backdoor variants. Specially, the average attack success rate can be reduced from 96.6% to 2.3% with only about 200 epochs.

2 Related Work

2.1 Backdoor Attacks on FL

Recently, many practical backdoor attacks on FL have been constructed. Wang et al. [Wang et al., 2020] firstly verify that adversarial examples can be used by edge-case backdoor attacks. Bagdasaryan et al. [Bagdasaryan et al., 2020] propose the first backdoor attack against FL, which selects specific semantics as the triggers for generating poisoned samples. Considering multiple colluding malicious clients, Xie et al. [Xie et al., 2020] formulate a distributed backdoor attack (DBA) method, in which each malicious client poisons local data with one kind of semantics and then forms a backdoored model that is only sensitive to the composited global trigger. Similarly, A.P. Sundar et al. [Sundar et al., 2022] utilize sizably-discrete local triggers to implant backdoors and validates its stealthiness using the DeepLIFT visual feature interpretation tool. Gong et al. [Gong et al., 2022] propose to use the model-agnostic triggers to increase the attack success rate of DBA. Zhang et al. [Zhang et al., 2022] find that tampering model parameters can improve the persistence of backdoor in FL. Xiao et al. [Xiao et al., 2022] demonstrate

that malicious clients also can create some Sybil nodes to manipulate the FL aggregation process, making the poisoned local models aggregated with higher probability.

2.2 Backdoor Purification for Trustworthy FL

Available backdoor purification methods mainly include two classes: **1) Backdoor diagnosis**. Unlike methods for preventing backdoor implantation, the goal of backdoor diagnosis is to determine whether a pre-trained model contains a backdoor. Neural Cleanse [Wang et al., 2019] identifies hidden backdoors by clustering the reconstructed triggers of each class. Qiao et al. [Qiao et al., 2019] improve the performance of Neural Cleanse by recognizing the possible distribution space of triggers. **2) Backdoor erasing**. Authors in [Li et al., 2021; Yan et al., 2023] propose to distillate a clean student model from the backdoored model. However, in FL, due to inaccessibility of clean samples, the convergence speed of backdoor erasing is too slow to adapt to the model aggregation process.

We observe that the reason why existing defences can not perform well in real FL scenarios is that backdoor prevention, backdoor deactivation and backdoor erasing are independent with each other. To swiftly sanitize hidden backdoors without training samples, more powerful black-box backdoor purification methods should be appreciated. Therefore, in this paper, we conduct the data-free and swift backdoor purification (DSBF) scheme based multi-teacher adversarial distillation, which puts backdoor diagnosis and erasing into a unified pipeline.

3 Data-free and Swift Backdoor Purification

In FL, the adversaries may design adaptive attacks to bypass existing backdoor purification. Therefore, to conduct a more powerful and efficient method that can purify hidden backdoors in a black-box way, we firstly identify the attacker’s possible intentions. Subsequently, we present the defender’s expectations and introduce the framework of proposed DSBP.

3.1 Attacker’s Intentions

We have the below assumptions for attacker’s intentions according to Fang et al. [Fang et al., 2020]: i) They can arbitrarily manipulate its local training data and model updates to implant backdoors once a client is captured. ii) They can reconfigure local training settings (e.g., the learning rate and the number of training iterations). Malicious clients do not know benign clients’ settings, but attackers can assume that defense strategies exist in the FL system and deploy corresponding evasion methods [Wang et al., 2020; Bhagoji et al., 2019; Ning et al., 2022]. Besides, since the stochastic gradient descent may monotonically decrease the loss function, the accuracy of intermediate global model gradually increases along with the model training rounds. Therefore, an additional basic assumption can be established: For any input x , $Acc(f_{\theta}^{r+1}(x)) > Acc(f_{\theta}^r(x))$, which means that using f_{θ}^{r+1} as a teacher model will distill a better student model S^{r+1} . And also, data samples reconstructed from f_{θ}^{r+1} will have higher quality. Specially, the teacher models in DSBP are denoted as $\mathcal{T}_s = f^{r+k}$ and $\mathcal{T}_w = f^r$, respectively.

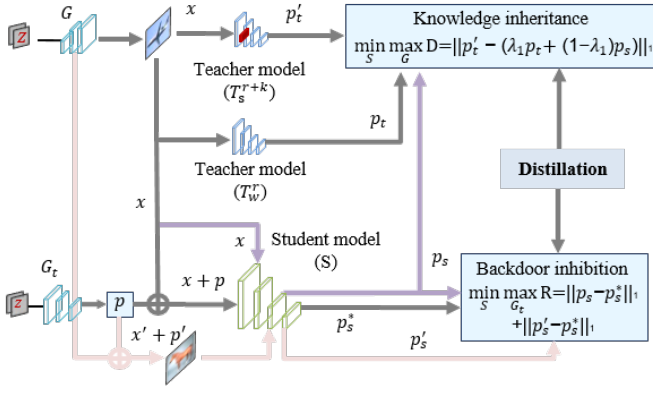


Figure 1: The proposed DSBP scheme. An adversarial game between knowledge inheritance and backdoor inhibition is illustrated. The knowledge inheritance is designed to transfer the teacher models’ reactions to the student model. Only when the T_w is backdoored, the student model will learn both normal reactions and backdoor reactions. Backdoor inhibition is designed to suppress the sensitivity of the student model to backdoor triggers, where \mathcal{R} is minimized.

3.2 Defender’s Expectations

Instead of adopting the previous popular settings [Wang *et al.*, 2019; Qiao *et al.*, 2019; Li *et al.*, 2021; Chen *et al.*, 2019b] where model updates are accessible, and also different from the settings in [Yan *et al.*, 2023] where only the backdoored model acts as the teacher model, we study a more practical setting, where the defender only can receive the delivered global models in each training round but does not have the ability to access model updates to execute model diagnosis. And also, it can not obtain clean samples to fine-tune the delivered global models. Formally, the delivered global model at the training round $r+k$ is denoted as \mathcal{T}_s^{r+k} : $\mathcal{X} \mapsto \mathbb{R}^{n_c}$, which takes image x with size $H \times W \times C$ as inputs and output a class score vector $q \in \mathbb{R}^{n_c}$. Moreover, we use \mathcal{T}_w^r to denote the delivered global model at the training round r , which has the same input and output size. Usually, after k training rounds, the accuracy of \mathcal{T}_s^{r+k} is higher than that of \mathcal{T}_w^r . During the k training rounds, if there are some malicious clients that have submitted poisoned updates to backdoor the FL-based system, the \mathcal{T}_s^{r+k} will be backdoored. In this case, \mathcal{T}_s^{r+k} predicts the poisoned images as the attacker-specified label y_p . The defender’s goal is to transform the knowledge of teacher models \mathcal{T}_s^{r+k} and \mathcal{T}_w^r into a clean student model \mathcal{S} without transferring hidden backdoors.

3.3 Multi-teacher Adversarial Distillation

We emphasize here the superiority of proposed DSBP via multi-teacher adversarial distillation (MAD) in real FL scenarios. **1) Better match with actual needs:** In many real-world cases such as face recognition, medical diagnosing, and so on, the defender does not want to erase backdoors frequently due to the high overheads and adverse effects on model accuracy. Our methods make it possible for the defender to swiftly construct a clean student model without accessing to clean samples and sacrificing model accuracy. Therefore, the DSBP will be more popular for large-scale

deployments in real FL-based systems. **2) scalable and independent:** Previous methods mainly use clean samples to fine-tune the backdoored model, but their performance may severely decrease if the attacker uses complex triggers [Xie *et al.*, 2020]. Our method can adaptively inverse various trigger variants by updating the trigger generators. Therefore, we believe our work will obtain rapid practical deployments.

In this subsection, we will further clarify the workflow of MAD. The backdoored model \mathcal{T}_s^{r+k} and \mathcal{T}_w^r are distilled into a clean student model \mathcal{S} , where the generalized objective function of MAD is formulated as:

$$\begin{aligned} \mathcal{S} &= \operatorname{argmin}_S \mathcal{L}(\mathcal{T}_s^{r+k}, \mathcal{T}_w^r, \mathcal{S}) \\ &= \operatorname{argmin}_S \mathcal{D}(\mathcal{T}_s^{r+k}, \lambda_1 \mathcal{T}_w^r + (1 - \lambda_1) \mathcal{S}) + \lambda_2 \mathcal{R}(\mathcal{S}) \end{aligned} \quad (1)$$

The first term $\mathcal{D}(\mathcal{T}_s^{r+k}, \lambda_1 \mathcal{T}_w^r + (1 - \lambda_1) \mathcal{S})$ is designed to measure the discrepancy between outputs of \mathcal{T}_s^{r+k} and the ensemble results of \mathcal{S} and \mathcal{T}_w^r , therein λ_1 is a hyper-parameter that should be carefully adjusted. Minimizing this discrepancy is equivalent to transferring the knowledge of \mathcal{T}_s^{r+k} and \mathcal{T}_w^r to \mathcal{S} . Compared to previous data-free distillation strategies, the additional teacher model \mathcal{T}_w^r has two important functions: 1) Accelerating knowledge inheritance, 2) Tracing the poisoned training rounds. The second term $\mathcal{R}(\mathcal{S})$ is a inhibition term that tries to restrain possible backdoors in \mathcal{S} . By jointly minimizing these two terms using a MAD mechanism, we can distill a clean student model that absorbs the teacher’s knowledge but discards backdoor reactions. In DSBP, we design two adversarial processes to simultaneously optimize \mathcal{D} and \mathcal{R} . Two adversarial processes are respectively denoted as: 1) *knowledge inheritance* and 2) *backdoor inhibition*.

Knowledge Inheritance (KI)

We utilize two intermediate global models to teach the student model, achieving high accuracy on clean samples. Four possible situations are considered: 1) Both \mathcal{T}_s^{r+k} and \mathcal{T}_w^r are backdoored, 2) Only \mathcal{T}_s^{r+k} is backdoored, 3) Both \mathcal{T}_s^{r+k} and \mathcal{T}_w^r are clean, 4) Only \mathcal{T}_w^r is backdoored. Intuitively, the student model \mathcal{S} is optimized to mimic the output of the teacher models according to the principle of knowledge distillation. Instead of using clean training data as inputs of all participation models, we design a sample generator $G: \mathbb{R}^n \mapsto \mathcal{X}$ to dynamically generate false training samples that can make the discrepancies between \mathcal{T}_s^{r+k} and $\lambda_1 \mathcal{T}_w^r + (1 - \lambda_1) \mathcal{S}$ be larger during the training process. Meanwhile, the student model \mathcal{S} adversarially updates itself to minimize the discrepancy on the generated false samples. In our KI framework, the discrepancy between \mathcal{T}_s^{r+k} and $(1 - \lambda_1) \mathcal{S} + \lambda_1 \mathcal{T}_w^r$ is optimized by the Mean Absolute Error (MAE) of model’s pre-softmax outputs over randomly-generated false samples. The discrepancy is shown as follows:

$$\begin{aligned} \mathcal{D}(\mathcal{T}_s^{r+k}, \mathcal{T}_w^r, \mathcal{S}; G) &= E_{z \sim p_z(z)} \left[\left\| \mathcal{T}_s^{r+k}(G(z)) - [(1 - \lambda_1) \right. \right. \\ &\quad \left. \left. \mathcal{S}(G(z)) + \lambda_1 \mathcal{T}_w^r(G(z))] \right\|_1 \right] \end{aligned} \quad (2)$$

where z is a random noise sampled from the normal distribution. In KI, both \mathcal{T}_s^{r+k} and \mathcal{T}_w^r are fixed, while G and \mathcal{S}

279 are updated to optimize Eq.1 respectively. Once \mathcal{S} catches up
 280 with the teachers over currently generated false samples, G
 281 will move forward to the next available space. For Situation
 282 1), two teacher models are backdoored so that G may gener-
 283 ate trigger-implanted false samples and transfer the back-
 284 doors into the student model. For Situation 2), the hidden
 285 backdoors in \mathcal{T}_w^{r+k} are forgotten if a small λ_1 is configured.
 286 For Situation 3), a clean \mathcal{S} will be achieved. For Situation 4),
 287 \mathcal{S} will also be backdoored when $\lambda_1 \mapsto 0$, but it can not be
 288 backdoored if $\lambda_1 \mapsto +\infty$. In summary, we can get a clean \mathcal{S}
 289 by adjusting the size of λ_1 except for Situation 1). In the next
 290 subsection, we will introduce how to comprehensively purify
 291 the backdoor reactions in Situation 1) using the Eq.3.

292 Backdoor Inhibition (BI)

293 In data-free scenario, we need retrieve the production of sam-
 294 ple space \mathcal{X} and trigger space Σ if we want the adversarial
 295 process between KI and BI to converge. However, directly
 296 optimizing this adversarial process is extremely difficult be-
 297 cause the production of these two spaces is too large. To pre-
 298 vent from transferring backdoor reactions to \mathcal{S} , an intuitive
 299 method is to make \mathcal{S} exhibit strong robustness to the triggers
 300 with ℓ_1 distances. To speed up the trigger search process,
 301 we consider that in targeted backdoor attacks, once data from
 302 different classes are patched with triggers, they will all be
 303 classified into the target class, defining as the self-similarity
 304 of poisoned features. To this end, the student model is desig-
 305 nated to predict the same result for inputs x , $x+p$ and $x'+p$:

$$\begin{aligned} \mathcal{R}(\mathcal{S}) = \mathbb{E}_{x, x' \sim \mathcal{X}} & \left[\|\mathcal{S}(x) - \mathcal{S}(x+p)\|_1 \right. \\ & \left. + \lambda_3 \|\mathcal{S}(x'+p) - \mathcal{S}(x+p)\|_1 \right] \end{aligned} \quad (3)$$

306 where λ_3 is a hyper-parameter that can be used to adjust the
 307 convergence speed of BI.

308 3.4 Overall Training Process of DSBP

309 Based on the above analysis, the overall training process of
 310 proposed DSBP scheme is the combination of KI (Eq.2) and
 311 BI (Eq.3). We summarize the coupled training processes as a
 312 whole objective function as follows:

$$\begin{aligned} \max_{G, G_t} \min_{\mathcal{S}} \mathcal{L}(\mathcal{T}_s^{r+k}, \mathcal{T}_w^r, \mathcal{S}, G, G_t) = \max_{G, G_t} \min_{\mathcal{S}} & \{ \mathcal{D}(\mathcal{T}_s^{r+k}, \\ & \mathcal{T}_w^r, \mathcal{S}; G) + \lambda_2 \mathcal{R}(\mathcal{S}; G_t) \} \end{aligned} \quad (4)$$

313 Here we take Situation 1) where both \mathcal{T}_s^{r+k} and \mathcal{T}_s^r are
 314 backdoored as an example. We initialize the student model
 315 is same with \mathcal{T}_s^{r+k} . And then, we sequentially train \mathcal{S} and
 316 simultaneously update the generators according to Alg. 1.

317 In each training round, we first update \mathcal{S} with k times
 318 (same as [Fang *et al.*, 2019] to achieve a stable G , we set
 319 $k = 5$ in all of our experiments) to optimize Eq.4. And then,
 320 G_t is updated to generate a trigger that can maximizes the
 321 backdoor redaction. Finally, we will update \mathcal{S} to make it be
 322 robust to all inputs.

323 4 Experiments

324 In this section, we first describe our experiment settings, and
 325 then we introduce the evaluation results of proposed DSBP

Algorithm 1: Training process of DSBP under Situation 2)

- 1: **Input:** A backdoored teacher model $\mathcal{T}_s^{r+k}(\cdot, \theta_t)$, batch size B , λ_1 , λ_2 , learning rates $\alpha_s, \alpha_g, \alpha_{gt}$, loss weight β_{gt} .
 - 2: **Output:** A clean student model $\mathcal{S}(\cdot, \theta_s)$.
 - 3: Initialize the student model's weights θ_s with θ_t .
 - 4: Randomly initialize the sample generator $G(\cdot, \theta_g)$ and the semantic trigger generator $G_t(\cdot, \theta_{gt})$.
 - 5: **for** The number of training iterations **do**
 - 6: **for** k steps **do**
 - 7: Randomly generate B samples $\{x_i\}$ and B triggers $\{p_i\}$ with G and G_p ;
 - 8: $\mathcal{L}_s = 1/B \sum_i (\|\mathcal{T}_s^{r+k}(x_i) - [(1 - \lambda_1)\mathcal{S}(x_i) + \lambda_1 \mathcal{T}_w^r(x_i)]\|_1 + \lambda_2 \|\mathcal{S}(x_i) - \mathcal{S}(x_i + p_i)\|_1)$;
 - 9: Update $\theta_s \leftarrow \theta_s - \alpha_s \nabla_{\theta_s} \mathcal{L}_s$;
 - 10: **end for**
 - 11: Randomly generate B samples $\{x_i\}$ with G ;
 - 12: $\mathcal{L}_g = -1/B \sum_i (\|\mathcal{T}_s^{r+k}(x_i) - [(1 - \lambda_1)\mathcal{S}(x_i) + \lambda_1 \mathcal{T}_w^r(x_i)]\|_1)$;
 - 13: Update $\theta_g \leftarrow \theta_g - \alpha_g \nabla_{\theta_g} \mathcal{L}_g$;
 - 14: Randomly generate B samples $\{x_i\}$ and B triggers $\{p_i\}$ with G and G_t ;
 - 15: $\mathcal{L}_{gt} = -1/B \sum_i \{ \|\mathcal{S}(x_i) - \mathcal{S}(x_i + p_i)\|_1 + \lambda_3 \|\mathcal{S}(x_i + p_i) - \mathcal{S}(x'_i + p_i)\|_1 \}$;
 - 16: Update $\theta_{gt} \leftarrow \theta_{gt} - \alpha_{gt} \nabla_{\theta_{gt}} \mathcal{L}_{gt}$
 - 17: **end for**
-

scheme against the well-known backdoor attacks on FL and compare the achieved effects with state of the art backdoor defence methods.

4.1 Experimental Settings

Basic experiment settings for running environments is configured as the same with [Yan *et al.*, 2023], including default parameters such as batch size, learning rate, client number, trigger size, available model structures. The biggest difference is that this article focuses on FL attack and defense, thus the pending-purified victim models are pre-trained using the state of the art attacks on FL introduced in 4.1.

Benchmark Datasets

Three standard image datasets are employed to evaluate the proposed framework, including MNIST, CIFAR10 and Mini-ImageNet.

Backdoor Attack Settings

We employ three typical backdoor attacks on FL with different backdoor injecting mechanism: model scaling [Bagdasaryan *et al.*, 2020], DBA [Xie *et al.*, 2020] and Neurotoxin [Zhang *et al.*, 2022]). We use 3 different size of triggers for each attack method. For a fair comparison, we re-implement these backdoor attacks and create backdoored models using the same Resnet-18 architecture provided by PyTorch. The total number of FL clients is configured as 100 and each epoch has less than 5 malicious clients. The scaling factor for all backdoor attacks is configured as 100. As a common practice for training small datasets with Resnet-18, the *conv1* layer (*kernal size* = 7, *stride* = 2) is replaced by *conv* (*kernal size* = 3, *stride* = 1) and the first *Pooling* layer is canceled to deal with inputs of size 32×32 (i.e. CIFAR10

Table 1: Comparison results of DSBP to data-driven and data-free purification methods on CIFAR10 dataset against different backdoor attacks and different size of triggers. Numbers are displayed as percentages.

Attack Methods	Trigger Size	Backdoored $t='truck'$		Finepruning $N_{clean} = 2000$		NAD $N_{clean} = 2000$		GDM $N_{clean} = 2000$		DHBE No data (r=1500)		DSBP No data (r=300)	
		ACC	ASR	ACC	ASR	ACC	ASR	ACC	ASR	ACC	ASR	ACC	ASR
Model scaling	2×2	84.75	98.92	82.70	12.8	82.75	0.38	77.92	0.25	83.05	1.2	83.77	0.25
	3×3	85.02	99.39	81.17	9.2	82.87	7.08	78.39	0.37	82.96	1.4	84.11	0.33
	5×5	85.11	99.28	81.96	57.8	82.41	8.76	78.21	0.46	83.24	1.7	83.88	0.27
Neurotoxin	2×2	64.85	96.32	63.49	17.5	60.28	1.22	56.39	0.92	63.19	1.1	63.49	0.56
	3×3	65.04	93.45	63.39	37.9	60.21	9.98	57.33	1.21	64.11	1.7	64.12	0.52
	5×5	68.82	99.00	64.74	54.1	60.69	9.57	58.08	0.68	65.45	1.4	64.02	0.54
DBA	1×4	77.91	91.60	68.65	12.6	71.24	0.4	67.57	0.03	74.96	1.8	75.11	0.38
	1×5	76.67	98.70	68.90	18.0	70.49	3.2	65.98	0.21	73.40	2.1	74.95	0.22
	1×6	75.58	92.87	67.79	53.4	70.67	5.6	64.88	0.23	72.58	2.4	72.52	0.12
Mean ACC/ASR		75.97	96.61	71.42	30.37	71.29	5.13	73.86	0.484	73.66	1.64	74.00	0.35

in our experiments). For inputs of size 64×64 (i.e. Mini-ImageNet in our experiments), the *conv1* layer is replaced by *conv* (*kernal size* = 5, *stride* = 2).

Configurations for Backdoor Purification Methods:

Available backdoor purification methods in FL mainly include data-driven and data-free methods. Fig. 2 illustrates the architectural comparison between data-free and data-driven methods. Three data-driven methods: 1) Finepruning [Liu *et al.*, 2018a], 2) NAD [Li *et al.*, 2021], and 3) GDM [Qiao *et al.*, 2019], are implemented as baselines. For these baselines, 4% of clean training *gsamples* (about 2000 samples) are available for the defender. Data-free method acting as baseline is DHBE [Yan *et al.*, 2023], which combines model inversion [Fredrikson *et al.*, 2015] with knowledge distillation [Chen *et al.*, 2019a]. However, DHBE requires at least 1000 rounds to reduce ASR to within 10%. Moreover, the effect of DHBE is extremely sensitive to its hyper-parameters. In DSBP, since two teacher models are used, more hyper-parameters are needed as illustrated in Eq. 1 and Eq. 3. Therein, λ_2 is inherited from the DHBE and we configure λ_2 as 0.1 in all experiments. **The λ_1 is a new hyper-parameter that enables the student model to imitate the updating process of the teacher model, rather than inherit the knowledge of the teacher model.** Further analysis about λ_2 is included in ablation experiments. λ_3 is another new hyper-parameter, controlling the convergence speed of proposed DSBP. For the optimizer, we globally employ an SGD optimizer with initial learning rate of 0.1, momentum of 0.9, and weight decay of $5e - 4$ to update the student model, and use an Adam optimizer with initial learning rate of $1e-3$ to update two different generators. The student model and the generators are jointly optimized for 50 iterations \times 200 epochs, where the student is updated by five times and generators are updated once in one iteration. 128 fake samples and triggers are generated in each iteration. The learning rates of SGD optimizer and Adam optimizer are decayed by 0.1 at epoch 180 and 240, respectively.

4.2 Purifying Hidden Backdoors

Since the effectiveness of data-driven methods depends on how confident the defender is that the given model contains

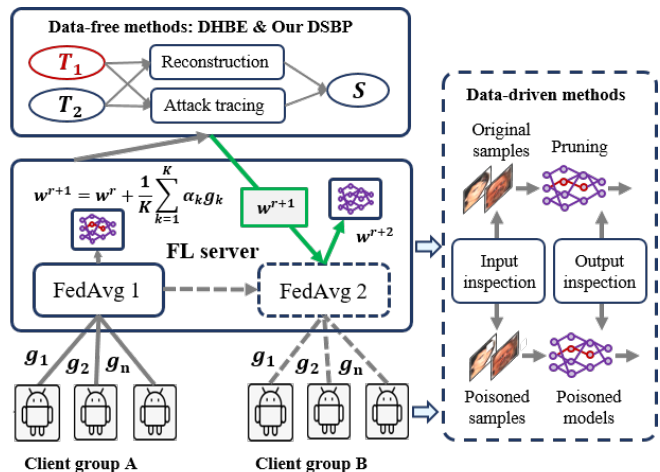


Figure 2: Architectural comparison between data-free sanitizing methods and data-driven sanitizing methods in FL. Data-free sanitizing methods are dominated by the FL server and can work well without accessing to original samples.

backdoor, we omit their backdoor diagnosing process and directly observe and report their backdoor purification performance. As for the comparison to existing data-free method, we focus on discussing hyper-parameter selection and convergence speed. Our experimental results show that the proposed DSBP scheme demonstrates superior performance than both data-driven and data-free methods.

Comparison with Data-driven Methods

Comparison results of our framework with data-driven methods on different backdoor attacks are shown in Table 1. It shows that the DSBP outperforms data-driven methods by a large margin on all kinds of backdoor attacks: The DSBP only slightly degrades the performance of the original model (about 1.97%), and reduce the attack success rate of all triggers to nearly neglectable. In contrast, the results of Finepruning, and NAD has about 4.5% accuracy degradation when the learning rate is set to 0.01. Under this setting, the backdoor purification effectiveness of Finepruning is unstable and failed to suppress ASR below 10% on some triggers. The

415 results of NAD perform better under multiple scenarios, the
 416 ASRs of most triggers are suppressed below 10%, but NAD
 417 still requires clean samples. The GDM achieves much better
 418 results than NAD and finepruning methods since it conducts
 419 the recovering routines of different triggers and then specifi-
 420 cally erases the hidden backdoor. But the robustness of trig-
 421 gers recovered in GDM can not be guaranteed due to data
 422 imbalance in FL. Despite the above weak performance, the
 423 effectiveness of data-driven methods is extremely sensitive to
 424 hyperparameters and the quantity of the clean dataset.

425 **a) Data-driven methods become less effective as the**
 426 **trigger invisibility increases.** We define three invisibility
 427 levels for triggers in backdoor attacks: 1) Low invisibil-
 428 ity: All malicious clients use the same trigger and samples
 429 patched with such trigger is easily detected using outlier de-
 430 tection or visual verification. 2) Medium invisibility: Each
 431 malicious client uses customized triggers, and only the global
 432 trigger can activate hidden backdoors, rendering client-side
 433 detection methods ineffective. 3) High invisibility: Sample-
 434 specific triggers are used to implant backdoors into the FL
 435 model. This level of invisibility usually requires the use of
 436 advanced data analysis and model detection techniques, as
 437 well as highly specialized and in-depth domain knowledge to
 438 be detected and identified. Figure 3 illustrates the triggers
 under different invisibility levels.

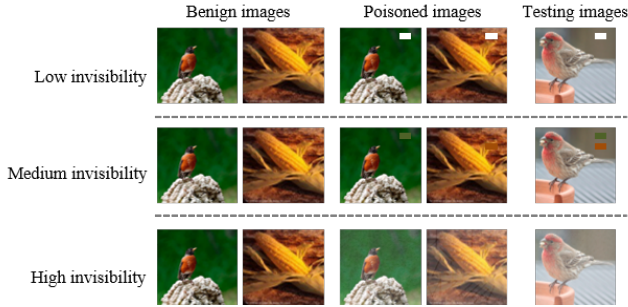


Figure 3: Illustration of our experimental settings with different trigger invisibility levels.

439 To visually present the relationship between trigger invis-
 440 ibility and defense effectiveness, we use “0”, “1” and “2” to
 441 represent the invisibility levels. Fig. 4 shows the records of
 442 ASR after deploying different data-driven methods. When
 443 there is no defense strategy, the ASR of backdoor attacks can
 444 exceed 96% using any form of trigger. However, as the invis-
 445 ibility of triggers increases, the effectiveness of data-driven
 446 methods decreases. Moreover, this decline in effectiveness is
 447 pronounced on complex datasets.

449 **b) Data-driven methods are extremely sensitive to the**
 450 **learning rate and the quantity of the clean dataset.** Since
 451 the DBSP is extended from DHBE, basic comparison exper-
 452 iments on this point can refer to [Yan *et al.*, 2023] for saving
 453 the texture space. The DSBP scheme is insensitive to hy-
 454 perparameters (e.g., the learning rate, λ_1 , and λ_2) due to its
 455 adversarial design, being demonstrated in ablation studies.

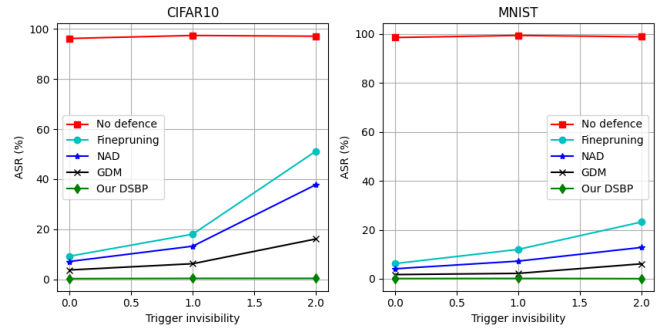


Figure 4: Effectiveness comparison with data-driven methods on MNIST and CIFAR10. As the invisibility of triggers increases, the effectiveness of data-driven methods decreases.

Comparison with Data-free Methods

456 Data-free backdoor purification method has not been widely
 457 studied yet. We only compare with DHBE [Yan *et al.*, 2023].
 458 As \mathcal{S} and \mathcal{G}_t are updated adversarially and simultaneously,
 459 all triggers that can be generated by \mathcal{G}_t will be mitigated. In
 460 DSBP, the \mathcal{G} is optimized using [Chen *et al.*, 2019a] and \mathcal{G}_t
 461 is optimized using Eq. 3. With these tricks, the distribution
 462 of generated samples is more equilibrium and the quality of
 463 generated data is also more real. the DSBP has comparable
 464 performance with DHBE under FL scenarios for the whole
 465 training process of DSBP only needs 200 epochs.

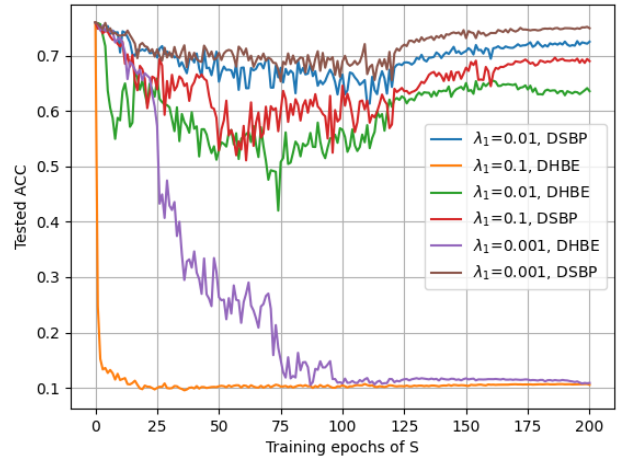


Figure 5: Robustness of DSBP to λ_1 against DHBE.

466 Moreover, we also compare the robustness of DHBE and
 467 DSBP to hyper-parameter λ_1 . In this experiment setting, we
 468 select two DBA pre-trained models as the strong teacher \mathcal{T}_s
 469 and the weak teacher \mathcal{T}_w , the weak teacher is not backdoored
 470 and also acts as the student model \mathcal{S} . λ_2 is configured as 0.1
 471 for all testings. Specially, we do not use any boosting strate-
 472 gies on DHBE as the baseline. Figure 5 shows the compar-
 473 ison results between DSBP and DHBE on robustness to λ_1 .
 474 Both $\lambda_1 = 0.1$ and $\lambda_1 = 0.001$ enforce the DHBE to be un-
 475 available. However, the performance of the proposed DSBP
 476 increases as λ_1 decreases, making the parameter conditions
 477 easier and more interpretable.
 478

4.3 Ablation Studies

In this subsection, we show that the effectiveness of the proposed DSBP is insensitive to a wide range of choices of hyperparameters, and DSBP is able to deal with backdoor attacks with different size of triggers using a same set of hyperparameters. These ablation studies suggest that our backdoor purification framework is robust enough and can be deployed in real-world applications with little trouble.

The effectiveness of ℓ_1 Vs. Smooth- ℓ_1

Seen from Table 1, both data-driven and data-free methods require additional 1500-2000 training rounds, which is impractical in actual federated learning scenarios, as we cannot wait for thousands of additional training rounds before proceeding to the next model aggregation. Intuitively, Eq. 7 is the key to sanitize the hidden backdoor, but using ℓ_1 as the loss function is difficult to balance the impact of outliers and noise on the distillation process, resulting in slow convergence speed. Fig. 6 compares the effect of backdoor inhibition under the scenarios of using Smooth- ℓ_1 and ℓ_1 , indicating that Smooth- ℓ_1 can achieve the accelerated backdoor inhibition.

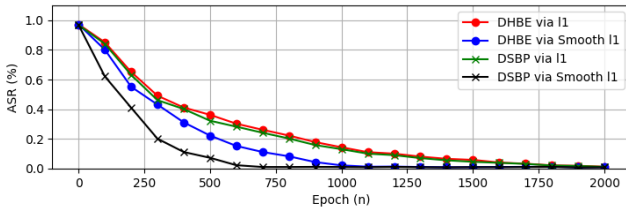


Figure 6: The ASR records with ℓ_1 and Smooth- ℓ_1 when $\lambda_3 = 0$.

Trigger size Vs. Convergence speed

Existing backdoor purification methods need to determine the shape, size, texture, and location of actual triggers, and commonly present better when the trigger size is smaller. For triggers with low invisibility level and medium invisibility level, when the trigger size increases from 2×2 to 5×5 , the effectiveness of all data-driven methods will decrease. For triggers with high invisibility levels, this weakness will extend to data-free methods. Authors of DHBE suggest that more neurons may be influenced by larger triggers, causing it hard to be erased by model unlearning and knowledge distillation. In contrast, the proposed DSBP framework appears to be more effective for larger triggers because the trigger generator in DSBP will try its best to produce larger triggers to cover the real triggers. In DBA, if the size of the local trigger on each malicious client is configured as 1×4 and the number of the triggers is configured as 4, then the global trigger size will be larger than 4×4 (actually it is often configured as $7 * 4$) because the minimum distance between each local trigger is 1. In our experiment, we use the coverage of the global trigger size by the noise size set on the generator as a metric to study the impact of trigger generator settings on defense effectiveness and model convergence speed. Table 2 presents the specific experimental results, which show that the size of the trigger has little effect on the defense effectiveness of DSBP, but the above coverage metric has a significant impact on model

convergence speed (named as ‘‘Conv’’), i.e., as the coverage increases, the convergence speed of DSBP increases. However, when the coverage exceeds 1, the convergence speed gradually decreases as the coverage increases.

Table 2: Comparison between different trigger generator settings. The trigger number is configured as 4 for all.

G_p	Local trigger	Min-area	Max-coverage	Conv
5×5	1×4	7×4	0.25	1200
	1×5	7×5	0.25	1500
	1×6	7×6	0	-
10×10	1×4	7×4	≥ 1	1000
	1×5	7×5	≥ 1	800
	1×6	7×6	≥ 1	500

The impact of λ_3 on DSBP

DSBP’s ability to quickly sanitize hidden backdoors is attributed to the self-similarity of poisoned features, which is weighted using λ_3 . In our experiments, we test the impact of λ_3 on the convergence speed of proposed DSBP scheme, and the results on different datasets are shown in Table 3. Three weight values of λ_3 are configured: 1) 0, 2) 0.1, 3) 0.3. It can be observed that the ASR discrepancy increases sharply as the value of λ_3 increases.

Table 3: The impact of λ_3 on DSBP over different datasets. The student model is trained with 200 epochs.

Datasets	λ_3	Acc	ASR	Discrepancy
MNIST	0	96.78	62.44	-34.66
	0.1	96.62	5.32	-91.78
	0.3	96.60	1.02	-96.08
CIFAR10	0	72.67	53.21	-43.47
	0.1	72.31	6.59	-90.1
	0.3	73.26	0.97	-95.71
Mini-Imagenet	0	73.59	54.93	-41.82
	0.1	73.77	6.82	-89.93
	0.3	73.52	1.21	-95.53

5 Conclusion

In this paper, a novel data-free and swift backdoor purification (DSBP) scheme based on multi-teacher adversarial distillation is proposed, which can effectively erase various backdoor variants in FL. The DSBP models the purification task as an adversarial game process between knowledge inheritance and backdoor inhibition, with the goal of enforcing the student model to learn the ensemble results of multiple teacher models on reconstructed clean samples, while being insensitive to synthetic poisoned samples. To accelerate the convergence of DSBP during the adversarial distillation process, we also propose to utilize the self-similarity of poisoned features to optimize the trigger generator. Extensive experiments based on 3 benchmark datasets against 4 state-of-the-art defense approaches over 3 backdoor variants demonstrate the effectiveness of proposed DSBP.

554 Acknowledgments

555 This research work is funded by the National Nature Science
556 Foundation of China under Grant No. 62202303, U21B2019,
557 and U20B2048, Shanghai Sailing Program under Grant No.
558 21YF1421700, Shanghai Municipal Science and Technology
559 Major Project under Grant 2021SHZDZX0102, and CCF-
560 AFSG RF20220018.

561 References

- 562 [Bagdasaryan and Shmatikov, 2020] Eugene Bagdasaryan
563 and Vitaly Shmatikov. Blind backdoors in deep learning
564 models. *arXiv preprint arXiv:2005.03823*, 2020.
- 565 [Bagdasaryan *et al.*, 2020] Eugene Bagdasaryan, Andreas
566 Veit, Yiqing Hua, Deborah Estrin, and Vitaly Shmatikov.
567 How to backdoor federated learning. *Proceedings of the*
568 *Twenty Third International Conference on Artificial Intel-*
569 *ligence and Statistics*, pages 2938–2948, 2020.
- 570 [Bhagoji *et al.*, 2019] Arjun Nitin Bhagoji, Supriyo
571 Chakraborty, Prateek Mittal, and Seraphin Calo. An-
572 alyzing federated learning through an adversarial lens.
573 *International Conference on Machine Learning (ICML)*,
574 pages 634–643, 2019.
- 575 [Chen *et al.*, 2019a] Hanting Chen, Yunhe Wang, Chang Xu,
576 Zhaohui Yang, Chuanjian Liu, Boxin Shi, Chunjing Xu,
577 Chao Xu, and Qi Tian. Data-free learning of student net-
578 works. In *IEEE/CVF International Conference on Com-*
579 *puter Vision (ICCV)*, pages 3513–3521, 2019.
- 580 [Chen *et al.*, 2019b] Huili Chen, Cheng Fu, Jishen Zhao, and
581 Farinaz Koushanfar. Deepinspect: A black-box trojan
582 detection and mitigation framework for deep neural net-
583 works. In *IJCAI*, 2019.
- 584 [Fang *et al.*, 2019] Gongfan Fang, Jie Song, Chengchao
585 Shen, Xinchao Wang, Da Chen, and Mingli Song.
586 Data-free adversarial distillation. *arXiv preprint*
587 *arXiv:1912.11006*, 2019.
- 588 [Fang *et al.*, 2020] Minghong Fang, Xiaoyu Cao, Jinyuan
589 Jia, and Neil Gong. Local model poisoning attacks to
590 Byzantine-Robust federated learning. In *USENIX Secu-*
591 *rity Symposium (USENIX Security 20)*, pages 1605–1622,
592 2020.
- 593 [Fredrikson *et al.*, 2015] Matt Fredrikson, Somesh Jha, and
594 Thomas Ristenpart. Model inversion attacks that exploit
595 confidence information and basic countermeasures. In
596 *CCS*, 2015.
- 597 [Goldblum *et al.*, 2022] Micah Goldblum, Dimitris Tsipras,
598 Chulin Xie, Xinyun Chen, Avi Schwarzschild, Dawn
599 Song, Aleksander Madry, Bo Li, and Tom Goldstein.
600 Dataset security for machine learning: Data poisoning,
601 backdoor attacks, and defenses. *IEEE Transactions on*
602 *Pattern Analysis and Machine Intelligence*, pages 1–1,
603 2022.
- 604 [Gong *et al.*, 2022] Xueluan Gong, Yanjiao Chen, Huayang
605 Huang, Yuqing Liao, Shuai Wang, and Qian Wang. Coor-
606 dinated backdoor attacks against federated learning with
607 model-dependent triggers. *IEEE network*, 36(1):84–90,
608 2022.
- [Hayase *et al.*, 2021] Jonathan Hayase, Weihao Kong, 609
Raghav Somani, and Sewoong Oh. Spectre: Defending 610
against backdoor attacks using robust statistics. In *ICML*, 611
2021. 612
- [Jia *et al.*, 2022] Jinyuan Jia, Yupei Liu, and Neil Zhenqiang 613
Gong. Badencoder: Backdoor attacks to pre-trained en- 614
coders in self-supervised learning. In *IEEE Symposium on* 615
Security and Privacy (SP), pages 2043–2059, 2022. 616
- [Kolouri *et al.*, 2020] Soheil Kolouri, Aniruddha Saha, 617
Hamed Pirsiavash, and Heiko Hoffmann. Universal litmus 618
patterns: Revealing backdoor attacks in cnns. In *CVPR*, 619
2020. 620
- [Li *et al.*, 2021] Yige Li, Xixiang Lyu, Nodens Koren, 621
Lingjuan Lyu, Bo Li, and Xingjun Ma. Neural attention 622
distillation: Erasing backdoor triggers from deep neural 623
networks. In *ICLR*, 2021. 624
- [Li *et al.*, 2022] Yiming Li, Yong Jiang, Zhifeng Li, and 625
Shu-Tao Xia. Backdoor learning: A survey. *IEEE Trans-* 626
actions on Neural Networks and Learning Systems, pages 627
1–18, 2022. 628
- [Lim *et al.*, 2020] Wei Yang Bryan Lim, Nguyen Cong Lu- 629
ong, Dinh Thai Hoang, Yutao Jiao, Ying-Chang Liang, 630
Qiang Yang, Dusit Niyato, and Chunyan Miao. Feder- 631
ated learning in mobile edge networks: A compre- 632
hensive survey. *IEEE Communications Surveys & Tutorials*, 633
22(3):2031–2063, 2020. 634
- [Liu *et al.*, 2018a] Kang Liu, Brendan Dolan-Gavitt, and 635
Siddharth Garg. Fine-pruning: Defending against back- 636
door attacks on deep neural networks. In *RAID*, 2018. 637
- [Liu *et al.*, 2018b] Yingqi Liu, Shiqing Ma, Yousra Aafer, 638
Wen-Chuan Lee, Juan Zhai, Weihang Wang, and Xiangyu 639
Zhang. Trojaning attack on neural networks. In *NDSS*, 640
2018. 641
- [Liu *et al.*, 2021] Xuankai Liu, Fengting Li, Bihan Wen, and 642
Qi Li. Removing backdoor-based watermarks in neural 643
networks with limited data. In *ICPR*, 2021. 644
- [Ning *et al.*, 2022] Rui Ning, Jiang Li, Chunsheng Xin, 645
Hongyi Wu, and Chonggang Wang. Hibernated backdoor: 646
A mutual information empowered backdoor attack to deep 647
neural networks. *Proceedings of the AAAI Conference on* 648
Artificial Intelligence, 36(9):10309–10318, Jun. 2022. 649
- [Qiao *et al.*, 2019] Ximing Qiao, Yukun Yang, and Hai Li. 650
Defending neural backdoors via generative distribution 651
modeling. In *NeurIPS*, 2019. 652
- [Sundar *et al.*, 2022] Agnideven Palanisamy Sundar, Feng 653
Li, Xukai Zou, and Tianchong Gao. Distributed swift and 654
stealthy backdoor attack on federated learning. In *2022* 655
IEEE International Conference on Networking, Architec- 656
ture and Storage (NAS), pages 1–8, 2022. 657
- [Wang *et al.*, 2019] Bolun Wang, Yuanshun Yao, Shawn 658
Shan, Huiying Li, Bimal Viswanath, Haitao Zheng, and 659
Ben Y Zhao. Neural cleanse: Identifying and mitigating 660
backdoor attacks in neural networks. In *IEEE S&P*, 2019. 661
- [Wang *et al.*, 2020] Hongyi Wang, Kartik Sreenivasan, 662
Shashank Rajput, Harit Vishwakarma, Saurabh Agarwal, 663

664 Jy-yong Sohn, Kangwook Lee, and Dimitris Papailiopoulos.
665 Attack of the tails: Yes, you really can backdoor
666 federated learning. *Advances in Neural Information*
667 *Processing Systems*, 33:16070–16084, 2020.

668 [Xiao *et al.*, 2022] Xiong Xiao, Zhuo Tang, Chuanying Li,
669 Bingting Jiang, and Kenli Li. Sbpa: Sybil-based backdoor
670 poisoning attacks for distributed big data in aiot-based fed-
671 erated learning system. *IEEE Transactions on Big Data*,
672 pages 1–12, 2022.

673 [Xie *et al.*, 2020] Chulin Xie, Keli Huang, Pinyu Chen, and
674 Bo Li. Dba: Distributed backdoor attacks against feder-
675 ated learning. *International Conference on Learning Rep-*
676 *resentations (ICLR)*, 2020.

677 [Xu *et al.*, 2021] Xiaojun Xu, Qi Wang, Huichen Li, Nikita
678 Borisov, Carl A Gunter, and Bo Li. Detecting ai trojans
679 using meta neural analysis. In *SP*, pages 103–120, 2021.

680 [Yan *et al.*, 2023] Zhicong Yan, Shenghong Li, Ruijie Zhao,
681 Yuan Tian, and Yuanyuan Zhao. Dhbe: Data-free holis-
682 tic backdoor erasing in deep neural networks via restricted
683 adversarial distillation. In *ACM ASIACCS*, 2023.

684 [Zhang *et al.*, 2022] Zhengming Zhang, Ashwinee Panda,
685 Linyue Song, and et al. Neurotoxin: Durable backdoors
686 in federated learning. In *International Conference on Ma-*
687 *chine Learning (ICML)*, volume 162, pages 26429–26446,
688 17-23 2022.